frontiers | Frontiers in Earth Science

ORIGINAL RESEARCH
published: 01 July 2022
doi: 10.3389/feart.2022.939372

Mechanical Properties and Acoustic Emission Characteristics of Weakly Cemented Sandstone With Different Grain Sizes

Bin Liu[1,2,3], *Tong Zhang*[2,3]*, *Hongwei Zhang*[3] *and Qiupeng Yuan*[1]*

[1]State Key Laboratory of Mining Response and Disaster Prevention and Control in Deep Coal Mines, Anhui University of Science and Technology, Huainan, China, [2]Institute of Energy, Hefei Comprehensive National Science Center, Hefei, China, [3]Engineering Research Center of Underground Mine Construction, Ministry of Education (Anhui University of Science and Technology), Huainan, China

The weakly cemented sandstone is widely distributed in the Western Mining Area, which is mainly formed by mineral grains and cemented minerals through compaction and cementation. To study the influence of grain size on the mechanical properties and acoustic emission (AE) characteristics of weakly cemented sandstone, uniaxial compression and Brazilian splitting AE tests were carried out on four weakly cemented sandstone specimens with different grain sizes. The physical properties, mechanical behaviors, and AE characteristics of sandstone under two conditions were analyzed, and the microfailure mechanism was investigated. The results show that the P-wave velocity, density, uniaxial compressive strength (UCS), and tensile strength of weakly cemented sandstones with different grain sizes decrease with the increase of grain size. The medium sandstone and coarse sandstone exhibit ductile failure, while the siltstone and fine sandstone exhibit brittle failure under the two conditions. The distribution of AE signal strength is nearly Gaussian in the time domain. The peak frequency and upper limit of signal strength are negatively correlated with grain size, and the occurrences of lots of high-strength AE signals can be used as the precursor of sandstone failure. The damage evolution shows the trend of low-speed damage-accelerated damage-low-speed damage, and the damage increase at the peak load is negatively related to the grain size. The microfailure mechanism is the tension-shear mixed failure, which is dominated by tensile failure, with few shear failures. The proportion of shear cracks is positively correlated with the grain size under uniaxial compression, while there is no significant correlation between shear cracks and grain size under Brazilian splitting.

Keywords: grain size, weakly cemented sandstone, acoustic emission (AE), signal strength, microfailure mechanism

OPEN ACCESS

Edited by:
Yulong Chen,
China University of Mining and Technology, China

Reviewed by:
Liang Xin,
Xi'an University of Technology, China
Shanjie Su,
Xuzhou University of Technology, China

***Correspondence:**
Tong Zhang
tzhang@aust.edu.cn
Qiupeng Yuan
2018100011@aust.edu.cn

Specialty section:
This article was submitted to Structural Geology and Tectonics, a section of the journal Frontiers in Earth Science

Received: *09 May 2022*
Accepted: *31 May 2022*
Published: *01 July 2022*

Citation:
Liu B, Zhang T, Zhang H and Yuan Q (2022) Mechanical Properties and Acoustic Emission Characteristics of Weakly Cemented Sandstone With Different Grain Sizes. Front. Earth Sci. 10:939372. doi: 10.3389/feart.2022.939372

INTRODUCTION

As the coal resource development strategy moves westward, the Western Mining Area has become the main coal production base in China. The weakly cemented sandstone is widely distributed in the shallow strata of the Western Mining Area, which is mainly formed by mineral grains and cemented minerals through compaction and cementation (Li and Li 2017; Zhao et al., 2019; Liu et al., 2021; Yang et al., 2021). The grain size and cementation degree of internal mineral grains have an obvious influence on their

physical properties and mechanical characteristics. Argillaceous cementation is the main form of weakly cemented sandstone, and the difference in its mechanical properties is mainly related to the grain size. Therefore, it is urgent to investigate the strength, deformation, and acoustic emission (AE) evolution of weakly cemented sandstone with different grain sizes, which is conducive to understanding the influence of grain size on the physical properties and mechanical behaviors of weakly cemented sandstone and is significant to the surrounding rock control of roadways in overlying strata in the Western Mining Area.

In recent years, many scholars have performed much research on weakly cemented rocks in the Western coal region and found that the mechanical characteristics of weakly cemented sandstone are easy weathering, large plastic deformation, strong anisotropy, low tensile and compressive strength, small internal friction angle and low cohesion. Li and Li (2017) analyzed the AE characteristics and mechanical characteristics of sandstone in the Shendong coalfield. Zhao et al. (2019) and Liu et al. (2021) investigated the mechanical properties, characteristic strength, and AE characteristics of weakly cemented rock at different buried depths in the Shendong coalfield. Wang et al. (2018) investigated the AE characteristics of weakly cemented sandstone with different bedding angles. You et al. (2018) analyzed the permeability capacity of weakly cemented sandstone under thermal and mechanical coupling, and Lyu et al. (2019) and Liu et al. (2020) studied the seepage capacity of weakly cemented sandstones. Song et al. (2020) determined the critical stress of weakly cemented sandstone by the renormalization group transformation rule. Bai et al. (2020) investigated the strength and deformation behaviors of weakly cemented red sandstone subjected to low-temperature freezing. Cai and Zou (2020) studied the failure characteristics and constitutive equation of weakly cemented sandstone under conventional triaxial compression. Wang et al. (2020) analyzed the correlation between the physical-mechanical properties and petrographic parameters for weakly cemented sandstones.

The mechanical properties of sandstone are greatly affected by grain size. Wasantha et al. (2015) and Yu et al. (2017, 2021) investigated the strain rate effect on deformation behaviors of sandstones with different grain sizes. Li et al. (2017) analyzed the microstructure characteristics of sandstones with different grain sizes. Atapour and Mortazavi (2018a, b) studied the average grain size effect on the uniaxial compressive strength (UCS) of weakly consolidated sandstones and the grain size and cement content effect on the physical properties and mechanical behaviors of weakly solidified artificial sandstones. Tian et al. (2018) investigated the crack propagation and coalescence of granite with different grain sizes under uniaxial compression. Jin et al. (2018) analyzed the physical properties and mechanical behaviors of grouted crushed coal with different grain sizes during the triaxial compression test. He et al. (2019) investigated the grain size and shape effect on strength according to fractal theory. Wu et al. (2020) studied the microstructure and deformation characteristics of sandstones with different grain sizes during the acid erosion test. Kong et al. (2021a, b) investigated the impact of grain size or anisotropy on the physical properties and mechanical behaviors of building stones and sandstone. Kang et al. (2021) analyzed the grain size effect on the strength of granite after high-temperature treatment. Carbillet et al. (2021) investigated the grain size and porosity effect on the mechanical compaction of crustal analogs. He et al. (2021) analyzed the influence of grain size on the microstructure characteristics of carbonate-based sand and silicate-based sand. The effect of grain size, mineralogy, and porosity on the mechanical properties of tight sandstones was also studied (Qi et al., 2022).

The above studies focus on the influence of grain size on the physical properties, deformation, failure, and seepage characteristics of hard rock and rock-like materials, while there are relatively few studies on the influence of grain size on the physical properties, deformation, failure, and seepage characteristics of weakly cemented sandstone. The overlying strata are usually in a state of compression, and local areas are in a state of tension during coal mining. As the tensile strength is much lower than the UCS, it is also necessary to study the tensile properties of the overlying strata. Therefore, it is necessary to investigate the strength, deformation, and failure characteristics of weakly cemented sandstone with different grain sizes under two mechanical properties (tension and compression). In this study, AE tests were conducted on four kinds of weakly cemented sandstones with different grain sizes (siltstone, fine sandstone, medium sandstone, and coarse sandstone) under uniaxial compression and Brazilian splitting. The physical properties, deformation, AE signal strength, and peak frequency of sandstones with different grain sizes under two conditions were analyzed, and the damage evolution and microfailure mechanism of sandstones were discussed. It provides basic parameters for pressure control and disaster prevention in the Western Mining Area.

MATERIAL AND TEST

Material Preparation

Four sandstones were collected from the geological borehole of the Buertai Coal Mine in the Shendong mining area of Inner Mongolia, with the buried depth of 300–400 m (Zhao et al., 2019; Liu et al., 2021). Four sandstone cores, coarse sandstone with a grain size of 0.50–1.00 mm, medium sandstone with a grain size of 0.25–0.50 mm, fine sandstone with a grain size of 0.10–0.25 mm, and siltstone with a grain size of 0.01–0.10 mm, were selected and processed into Brazilian disc (Φ 50 mm × 25 mm) and cylindrical samples (Φ 25 mm × 50 mm) due to the disintegration of weakly cemented sandstone cores. The two end faces of the rock samples should be polished to ensure that the roughness of the end faces is less than 0.1 mm. A nonmetallic ultrasonic tester (Model: ZBL-U510) was used to conduct axial P-wave velocity tests on rock samples, and the physical parameters of the rock samples are listed in **Table 1**.

Test Equipment

The testing machine (Model: WDW-100E) and multichannel AE monitoring instrument (Model: PCI-Express8) were used in this test (**Figure 1**). The axial load of the testing machine ranges from 0.40 to 100 kN, and the range of axial displacement is 0.2–100 mm. The maximum and minimum loading speeds are 500 mm/min and 0.005 mm/min, respectively. The load and displacement data in the loading process can be recorded

TABLE 1 | Physical and mechanical properties of rock samples.

Loading Form	Lithology	Sample no.	Density (g·cm^{-3})	P-Wave Velocity (m·s^{-1})	Compressive/Tensile strength (MPa)	Mean MPa
Uniaxial compression	Medium Sandstone	U221	2.17	1,145	4.29	5.96
		U222	2.16	1,220	5.63	
		U223	2.26	1,135	4.76	
		U224	2.23	937	9.15	
	Coarse Sandstone	U321	2.03	737	2.92	3.91
		U322	2.08	716	2.93	
		U323	2.07	703	3.57	
		U324	2.01	540	6.20	
	Siltstone	U511	2.55	2,248	34.59	31.87
		U512	2.54	2,121	38.43	
		U513	2.47	2,108	22.59	
	Fine Sandstone	U611	2.42	2042	26.81	26.58
		U612	2.41	1,995	28.50	
		U613	2.44	1,958	26.64	
		U614	2.40	1,830	24.38	
Brazilian splitting	Medium Sandstone	B031	2.05	998	0.30	0.25
		B032	2.09	991	0.19	
	Coarse Sandstone	B211	2.04	675	0.18	0.18
		B212	1.95	749	0.12	
		B213	1.95	654	0.24	
	Siltstone	B511	2.46	2,212	2.08	2.27
		B512	2.47	2,839	1.16[a]	
		B516	2.40	2,068	2.45	
	Fine Sandstone	B542	2.39	2,319	1.88	2.06
		B543	2.27	1,930	2.17	
		B545	2.29	1,678	2.15	

[a]*Due to the abnormal internal structure of the Brazilian disc B512, the P-wave velocity and tensile strength were abnormal, which were discarded when calculating the average tensile strength.*

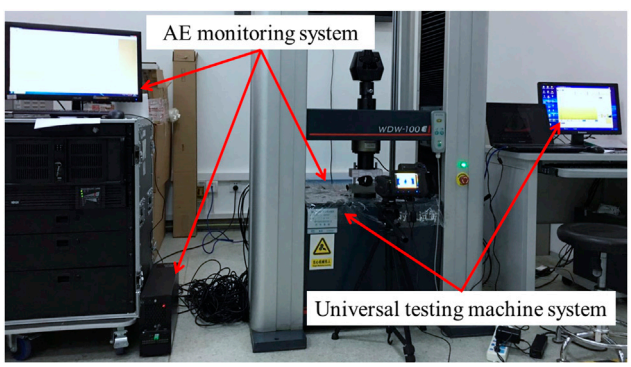

FIGURE 1 | Layout of the test device.

synchronously, and the load-displacement and load-time curves can be drawn synchronously. The AE monitoring instrument, equipped with eight AE sensors and amplifiers, can record and analyze the AE parameters in real-time. The center frequency of the AE sensors is 140 kHz, and the frequency range is 125–750 kHz.

Experimental Scheme

AE tests were conducted on four weakly cemented sandstone samples with different grain sizes under uniaxial compression and Brazilian splitting. The loading rates were set as 0.50 mm/min and 0.20 mm/min. The AE signals were acquired and stored synchronously during the loading process. As shown in **Figure 2**, two sensors were symmetrically arranged on the left and right sides of the rock sample under uniaxial compression, and four AE sensors were fixed on the back of the rock sample in the Brazilian splitting test. The signal threshold was fixed at 45 dB after measuring the ambient noise, and the sampling frequency was fixed at 1 MHz. The AE sensors were fixed on the surface of the rock sample with Vaseline to ensure contact between the AE sensor and the surface of the rock sample. Before the test, the samples were fixed on the fixture with an initial load of 0.01 kN. The testing machine system and AE monitoring instrument were synchronized during the test, and the load-displacement data and AE data were analyzed and summarized after the test.

RESULTS AND DISCUSSION

Physical Properties

The physical characteristics of the four weakly cemented sandstones, such as density and P-wave velocity, are significantly different due to the variation in grain size composition. **Figure 3** shows that the density of coarse sandstone is the lowest, with a distribution range of 1.95–2.08 g/cm^3 and an average of 2.01 g/cm^3, while the density of siltstone is the highest, with a distribution range of 2.38–2.55 g/cm^3 and an average of 2.48 g/cm^3, which is 1.23 times that of coarse sandstone. Similarly, the P-wave velocity of coarse sandstone is the lowest, with a distribution range of 540–749 m/s and an average of 682 m/s, while the density of siltstone is the highest, with a

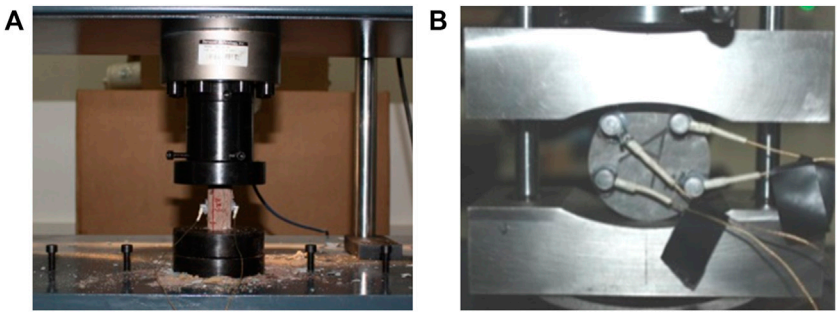

FIGURE 2 | Layout of AE sensors **(A)** uniaxial compression, **(B)** Brazilian splitting.

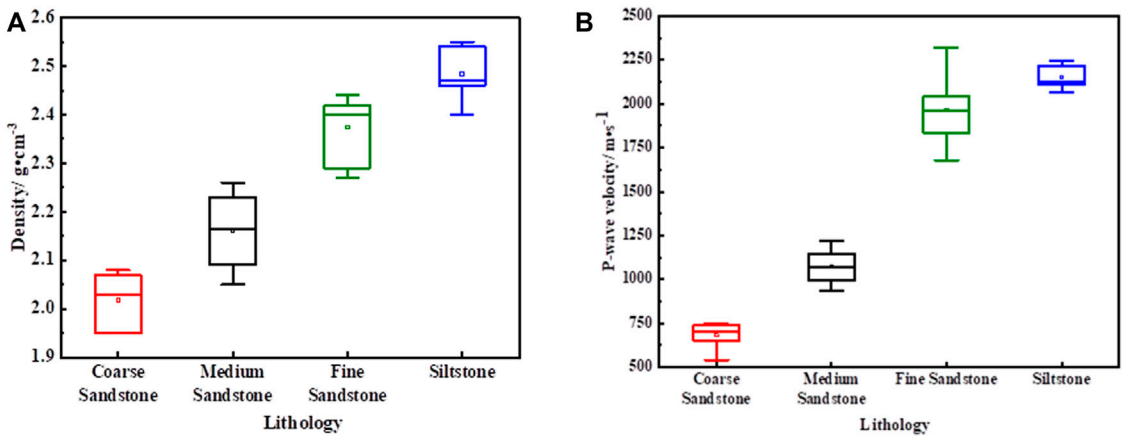

FIGURE 3 | Distribution of density and P-wave velocity for sandstone with different grain sizes **(A)** density, **(B)** P-wave velocity.

distribution range of 2,068–2,248 m/s and an average of 2,151 m/s, which is 3.15 times that of coarse sandstone. In summary, the density and P-wave velocity decrease with increasing grain size. The phenomenon indicates that the smaller the grain size is, the fewer internal pores and fissures there are, and the higher the density is. Similarly, there are some reflections and refractions when P-waves pass through fissures and pores, resulting in wave velocity reduction during the process of P-wave testing. The P-wave velocity of weakly cemented sandstone in this study is lower than 2,750 m/s, which is significantly lower than that of other hard sandstones (**Figure 3**). Due to the influence of the mineral composition and microstructure of sedimentary rocks, there is a certain variation in rock density and P-wave velocity, thus the density and P-wave velocity of some samples show great discreteness (Galouei and Fakhimi 2015).

The P-wave velocity is an important index to evaluate the quality of coal and rock. The relationship between density and P-wave velocity was obtained according to a large amount of measured data (Gardner et al., 1974), and the equation is as follows:

$$\rho = aV_P^b \quad (1)$$

where ρ is the density, g/m^3; V_P is the p-wave velocity, m/s; and a and b are constants.

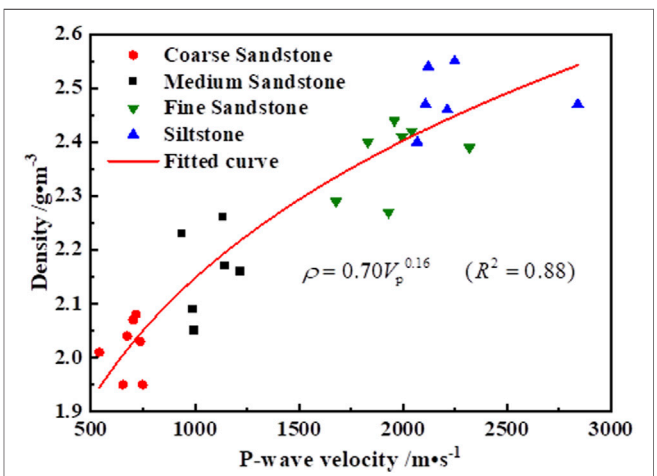

FIGURE 4 | Relationship between density of sandstone with different granularities and P-wave velocity.

According to the previous density-velocity formula, the fitting results are shown in **Figure 4**. On the whole, the density of rock samples increases with increasing P-wave velocity, which is consistent with the previous formula. However, there are obvious differences

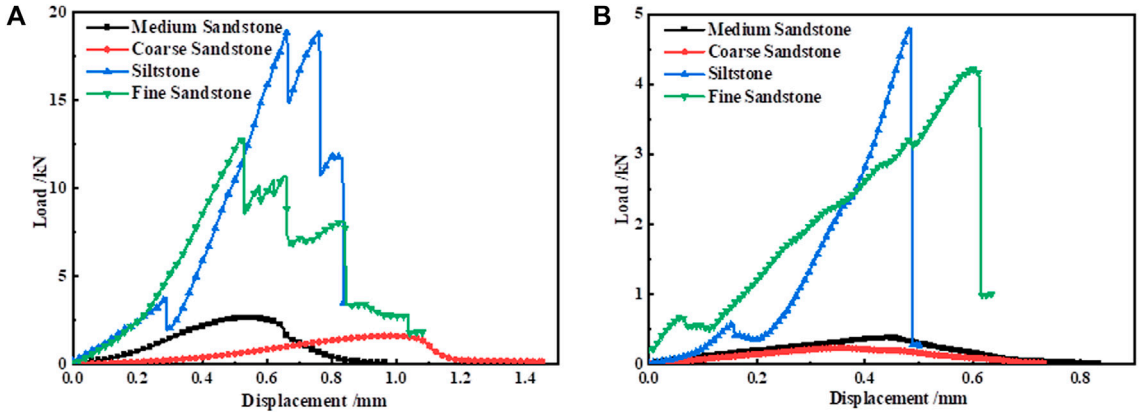

FIGURE 5 | Load-displacement curves of typical sandstone with different grain sizes **(A)** uniaxial compression, **(B)** Brazilian splitting.

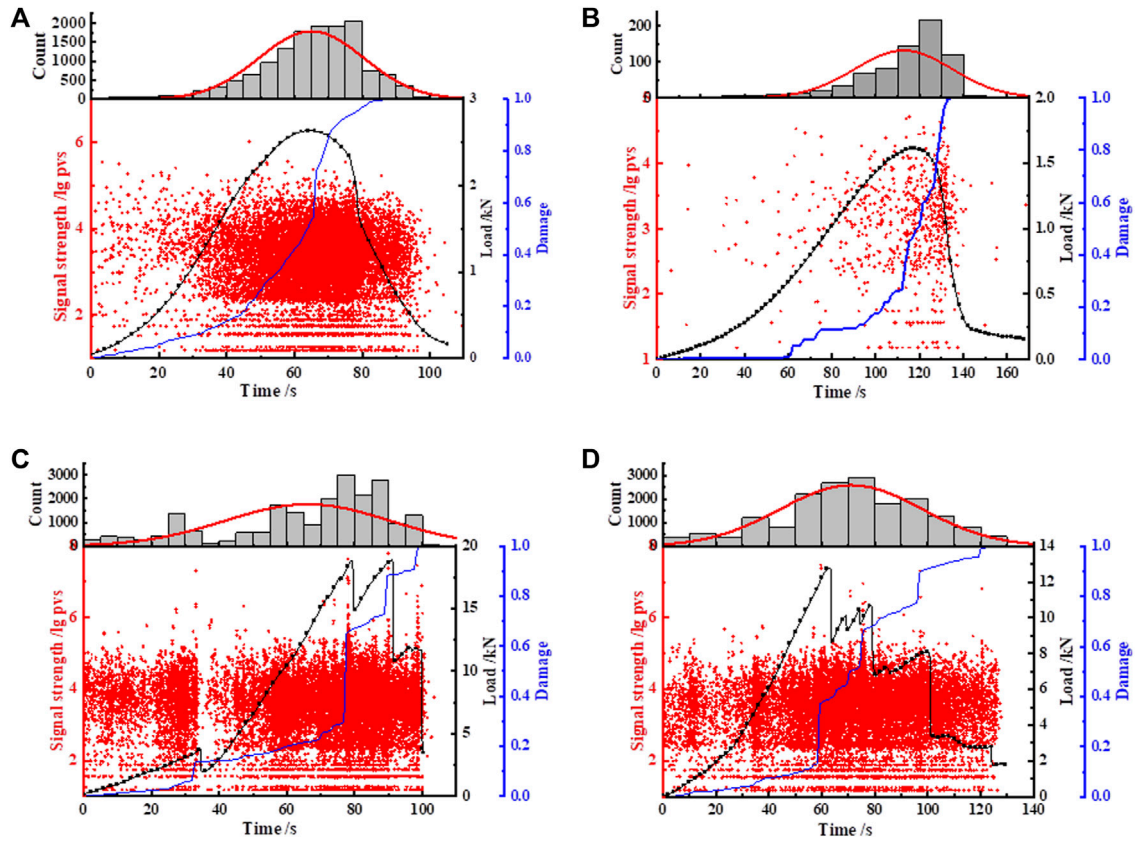

FIGURE 6 | Distribution of load, damage and signal strength for typical sandstone with different grain sizes under uniaxial compression **(A)** medium sandstone, **(B)** coarse sandstone, **(C)** siltstone, and **(D)** fine sandstone.

between parameters a and b, which are mainly caused by the differences in the composition and structure of sedimentary rocks.

Strength and Deformation Behaviors

According to the formulas of compressive and tensile strength, the calculation results are listed in **Table 1**. The compressive and tensile strength of coarse sandstone is the lowest, with an average value of 3.91 and 0.18 MPa. The compressive and tensile strength of siltstone is the highest, with average values of 31.87 and 2.27 MPa, which are 8.15 and 12.61 times those of coarse sandstone, respectively. The strength is consistent with previous research (Li et al., 2017; Li and Li 2017; Du and

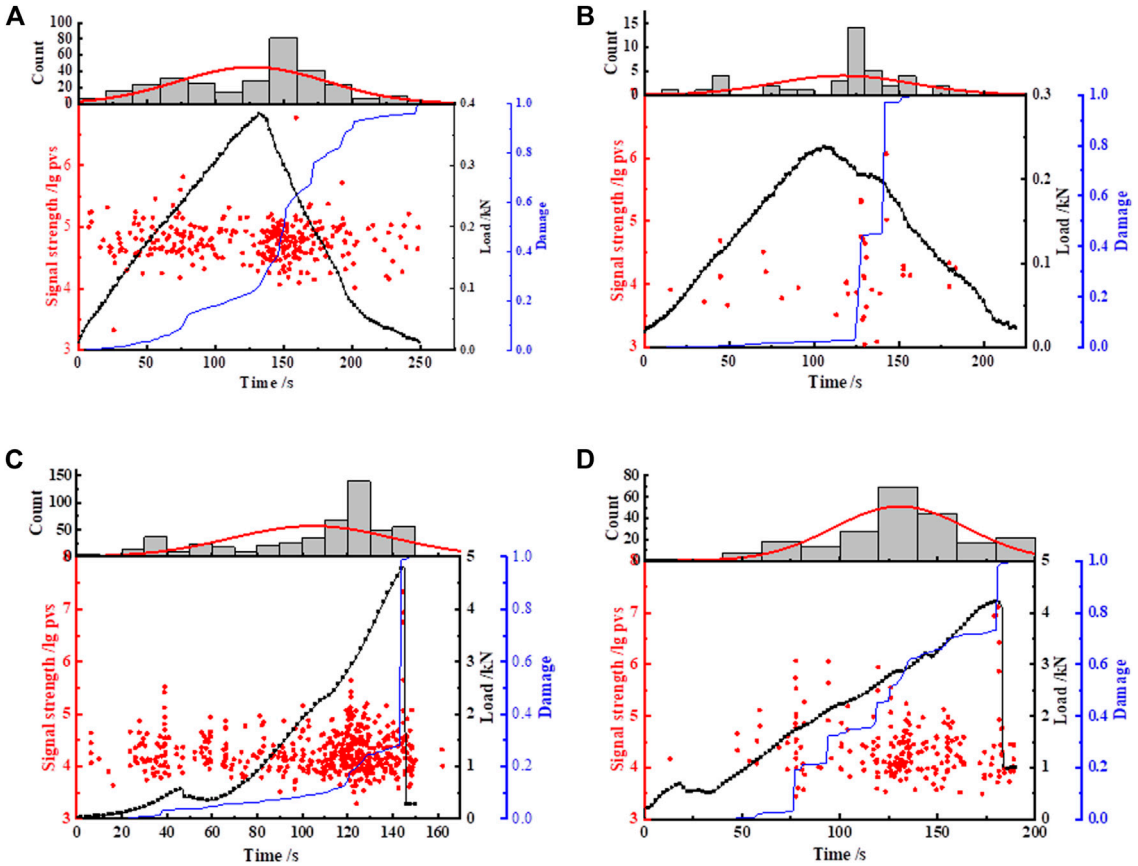

FIGURE 7 | Distribution of load, damage and signal strength for typical sandstone with different grain sizes under Brazilian splitting **(A)** medium sandstone, **(B)** coarse sandstone, **(C)** siltstone, and **(D)** fine sandstone.

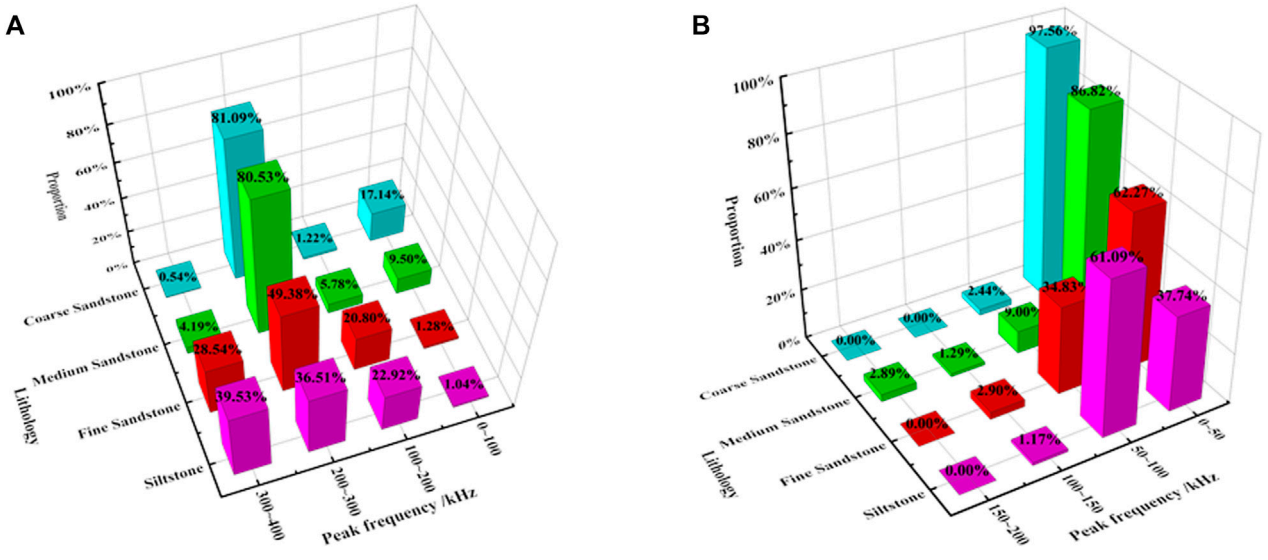

FIGURE 8 | Distribution of peak frequency for typical sandstone with different grain sizes **(A)** uniaxial compression, **(B)** Brazilian splitting.

Peng 2019) and far lower than that of other hard sandstones. In summary, both compressive and tensile strength is negatively correlated with grain size; that is, the smaller the grain size is the higher the compressive and tensile strength, which is consistent with existing research results (Zou et al., 2015). The reason is that the grain size of sandstone is smaller, the pores and fissures are fewer, the internal density is higher, and the degree of grain adhesion is stronger, so the compressive and tensile strengths are higher.

The load-displacement curves of typical sandstones with different grain sizes under uniaxial compression (**Figure 5A**). The pre-peak deformation characteristics of sandstones with different grain sizes are the same and can be divided into the primary fissure compaction stage, elastic stage, and yield stage (Hoek and Bieniawski 1984; Eberhardt et al., 1998; Chen et al., 2021). However, there are some differences in the post-peak stage. Siltstone and fine sandstone have several step-falls after the peak load, showing certain brittle failure characteristics. In contrast, the medium sandstone and coarse sandstone decrease slowly after the peak and show ductile failure characteristics. The reason is that the grain size is small, the pores and fissures are fewer, the internal density is high, the degree of grain adhesion is strong, and the energy storage capacity is strong, so the energy released after the peak is fast, showing certain brittle failure characteristics. However, other hard sandstones (Cheng et al., 2017) show strong brittle failure characteristics and sudden drops in the post-peak stage. This phenomenon indicates that there exists some plastic deformation after the peak stress under the external load, showing certain ductility failure characteristics, which are mainly caused by the low internal cementation degree of weakly cemented sandstone.

The load-displacement curves of typical sandstones with different grain sizes under Brazilian splitting (**Figure 5B**). The pre-peak deformation characteristics of sandstones with different grain sizes are the same and can be divided into the primary fissure compaction stage, elastic stage, and yield stage (Hoek and Bieniawski 1984; Eberhardt et al., 1998). There are also some differences in the post-peak stage; loads of siltstone and fine sandstone drop rapidly, showing certain brittleness characteristics. While a load of coarse sandstone and medium sandstone decreases slowly with increasing deformation after the peak load, the internal cracks continue to propagate and coalesce, and the rock samples gradually lose stability and fail, showing certain ductility characteristics. The main reason is that sandstone is a brittle material, and the tensile strength is much lower than the compressive strength. The sandstone with a small grain size is denser and more brittle, thus the load decreases faster under the tensile load during the post-peak stage, showing certain brittleness characteristics.

AE Signal Intensity and Peak Frequency Characteristics

The elastic energy is released to the surroundings in the form of AE signals during the whole loading process, and the AE signal can directly characterize the damage and failure evolution of coal and rock (Zhao et al., 2019; Dou et al., 2021; Liu et al., 2021). Therefore, the distribution of AE signal intensity and peak frequency was analyzed in this section. AE signal intensity is the mathematically defined as the integral of the rectified voltage signal over the duration of the AE waveform packet. This feature is similar to the AE energy feature, except that it is calculated over the entire AE signal dynamic range and independent of gain.

Figures 6, **7** show the distribution of AE signal intensity and peak frequency of sandstone with different grain sizes under the two conditions. The evolution of signal intensity under the two conditions is the same. At the initial phase of loading, few medium- and low-intensity AE signals are generated due to the closure of internal fissures and pores. With increasing load, internal microcrack initiation was accompanied by a small amount of crack propagation, resulting in more medium- and low-intensity AE signals and a small amount of high-intensity AE signals. A large number of medium- and high-intensity AE signals appear due to the rapid propagation and coalescence of cracks, accompanied by a small number of low-intensity AE signals near the peak load. Only a small amount of medium- and low-intensity AE signals are released after the peak load.

The AE signal intensity of sandstone with different grain sizes under the two conditions is concentrated between 3.5 and 4.5. The high-intensity AE signal (>4.5) gradually decreases with increasing intensity, and the low-intensity AE signal (< 3.5) gradually decreases with decreasing intensity. However, the range of signal intensity under the two conditions is different. The lower limit of signal intensity under uniaxial compression is 1.10, while the upper limit is 4.71 for coarse sandstone, 6.02 for medium sandstone, 7.48 for fine sandstone, and 7.80 for siltstone. The lower limit of signal intensity under Brazilian splitting is 3.10, while the upper limit of signal intensity is different, which is 6.07 for coarse sandstone, 6.77 for medium sandstone, 7.10 for fine sandstone, and 7.34 for siltstone. This phenomenon indicates that

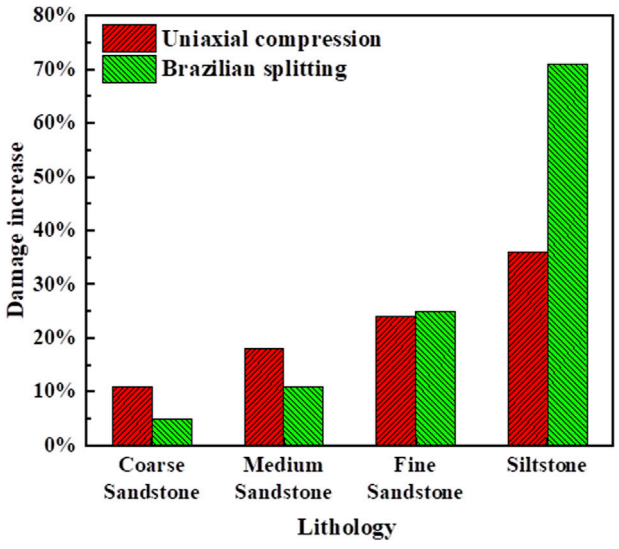

FIGURE 9 | Distribution of damage increase for typical sandstone with different grain sizes.

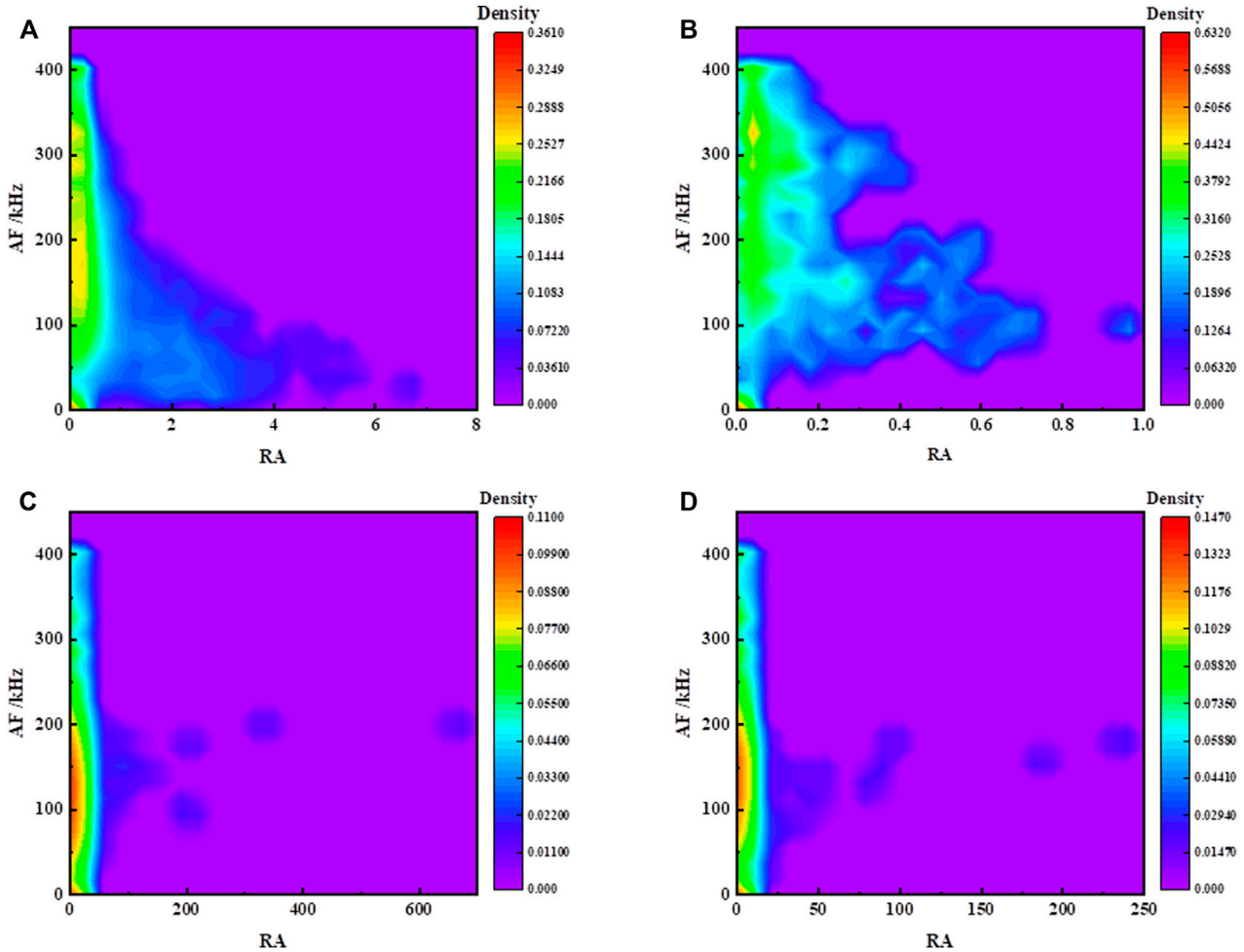

FIGURE 10 | AF-RA data density maps for typical sandstone with different grain sizes under uniaxial compression **(A)** medium sandstone, **(B)** coarse sandstone, **(C)** siltstone, and **(D)** fine sandstone.

the smaller the grain size is, the higher the upper limit of the signal intensity is, and the upper limit is negatively correlated with the grain size. The main reason is that the smaller the grain size is, the fewer pores and fissures between the grains, and the denser the microstructure is, the more strain energy stored before the peak load, the more severe the damage is, and the higher the AE signal intensity is. A large amount of high-intensity AE signals are generated in sandstone with different grain sizes near the peak load, which can be regarded as the failure precursor of sandstone.

As shown in **Figures 6**, **7**, the distribution of AE counts of sandstone with different grain sizes under the two conditions are the same. Only a small number of AE signals are generated at the initial phase of loading. With increasing load, the AE signals increase gradually. AE signals reach the peak value near the peak load and decrease gradually in the post-peak stage. Therefore, the AE signals present a nearly normal distribution in the time domain.

Figure 8 shows the distribution of the peak frequency for sandstone with different grain sizes under uniaxial compression and Brazilian splitting. As shown in **Figure 8A**, the peak frequency of sandstone ranges from 0 to 400 kHz and is concentrated on 200–300 kHz during the uniaxial compression test. The proportion of sandstone with different grain sizes at low frequencies (0–100 kHz) is positively correlated with grain size, while that at high frequencies (300–400 kHz) is negatively correlated with grain size. The reason is that the grain size is small, the microstructure is dense, and the AE frequency is high; that is, the low-frequency AE signal is less, and the high-frequency AE signal is more. However, sandstone with a larger grain size has more pores and fissures, and the AE frequency is low; that is, there are more low-frequency AE signals and fewer high-frequency AE signals. As shown in **Figure 8B**, the range of peak frequency for sandstone with different grain sizes is 0–200 kHz under Brazilian splitting, and the peak frequency is concentrated at 0–200 kHz. The proportion in the range of 0–50 kHz is positively correlated with grain size, while the proportion in the range of 50–100 kHz is negatively correlated with grain size. The reason is consistent with that under uniaxial compression.

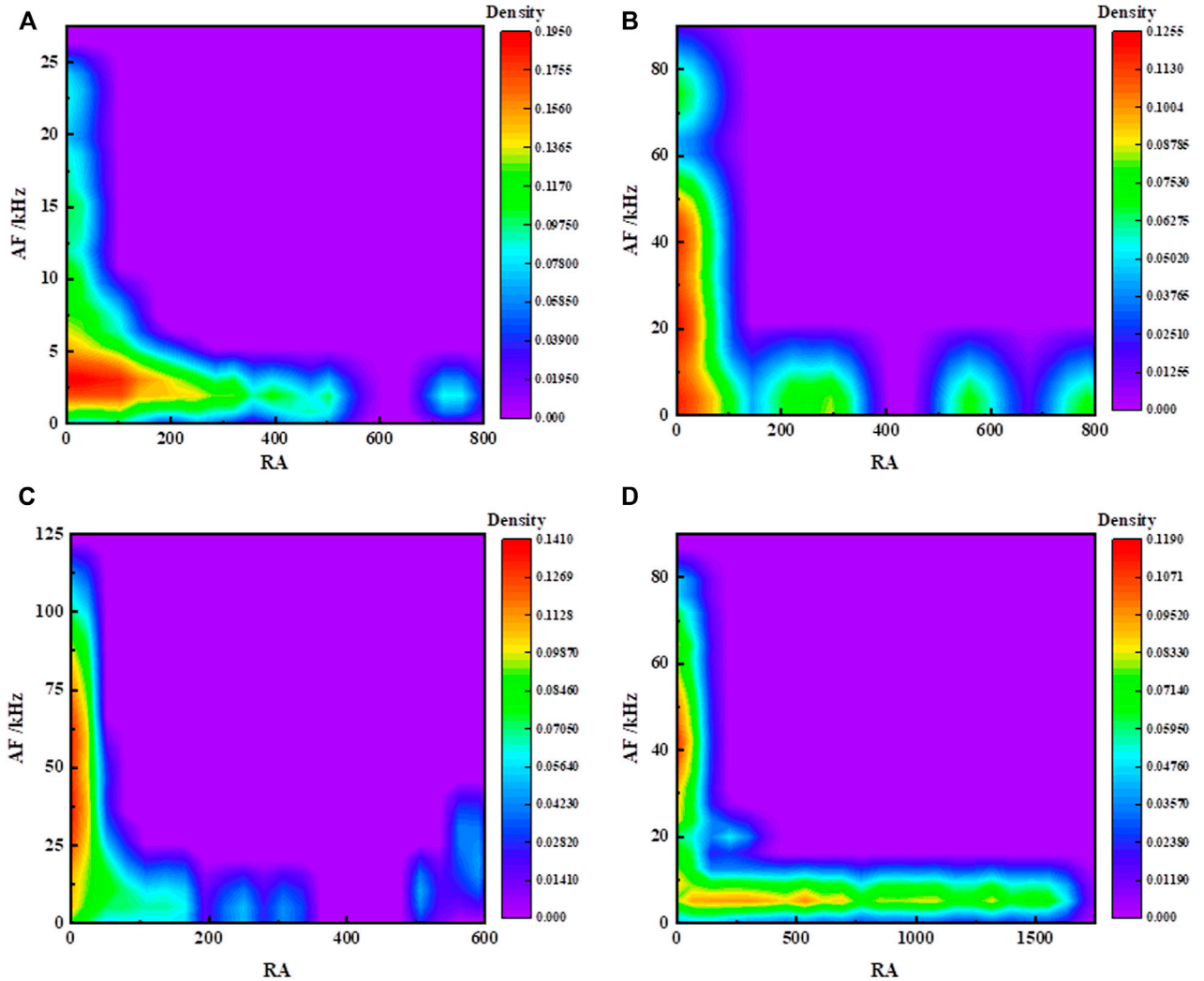

FIGURE 11 | AF-RA data density maps for typical sandstone with different grain sizes under Brazilian splitting **(A)** medium sandstone, **(B)** coarse sandstone, **(C)** siltstone, and **(D)** fine sandstone.

Damage Evolution

Relevant studies show that AE parameters can be used to quantitatively investigate the damage evolution of coal and rock (Liu et al., 2009; Zhao et al., 2019). In this study, the cumulative AE energy is used to define the damage variable during the loading process (Zhao et al., 2019). The damage variable D can be expressed as:

$$D = E_d / E_0 \tag{2}$$

where E_d is the cumulative AE energy at any time in the loading process and E_0 represents the cumulative AE energy corresponding to the moment of rock failure.

Figures 6, **7** also show the damage evolution curves of typical sandstones with different grain sizes under the two conditions, and the damage evolution of sandstones with different grain sizes is consistent. At the initial stage, damage variable D increases slowly due to the closure of internal fissures and pores. With increasing load, internal microcracks begin to appear, and the speed of damage increases rapidly. The damage increases suddenly near the peak load, and the damage increases slowly after the peak load. The damage shows the evolution of low damage - accelerated damage - low damage during the whole damage process.

Figure 9 shows the damage increases for coarse sandstone, medium sandstone, fine sandstone, and siltstone are 0.11, 0.18, 0.24, and 0.36 under uniaxial compression, and 0.05 for coarse sandstone, 0.11 for medium sandstone, 0.25 for fine sandstone and 0.71 for siltstone under Brazilian splitting. Namely, the larger the grain size of sandstone is, the lower the damage increase at the peak load, and the damage increase is negatively correlated with the grain size. This phenomenon implies that the grain size of sandstone is smaller, the pores and fissures are fewer, the internal density is higher, the degree of grain adhesion is stronger, and more energy is stored, so the damage at the peak load is more severe, and the damage increase is higher.

Microfailure Mechanism

Related studies have proved that the microfailure mechanism of coal and rock can be studied through AE waveforms. In general, the AE waveforms with low RA (rise time/amplitude) and high AF (count/duration) correspond to tension cracks, waveforms with high RA and low AF correspond to shear cracks, and waveforms with low RA and AF correspond to tension-shear mixed cracks (Aggelis 2011; Elfergani et al., 2013).

Figures 10, **11** show the AF-RA data density maps for typical sandstone with different grain sizes under uniaxial compression and Brazilian splitting. The high AF-RA data density area (red area) of sandstone with different grain sizes mainly appears near the longitudinal axis (low RA value) and at the origin of coordinates (low RA and low AF value), and few occur near the horizontal axis (low AF value). In summary, the microfailure mechanism of sandstone with different grain sizes under uniaxial compression and Brazilian splitting is the mixed failure of tensile and shear failure, which is dominated by tensile failure, with few shear failures.

As shown in **Figure 10**, the AF value distribution of sandstone with different grain sizes under uniaxial compression is the same, ranging from 0 to 400 kHz. However, RA values vary, ranging from 0 to 1 for coarse sandstone, 0 to 8 for medium sandstone, 0 to 250 for fine sandstone, and 0 to 700 for siltstone. The main reason is that the larger the grain size of sandstone is, the more defects such as internal fissures and pores, the stronger the friction effect under an external load, and the lower the RA value. Therefore, the determination of crack types based on AF/RA should be based on the actual AE signal distribution due to the differences in RA values for different types of coal and rock. However, there are significant differences in the proportion of shear cracks for sandstone with different grain sizes: coarse sandstone >medium sandstone >fine sandstone >siltstone. The reason is that the larger the grain size of sandstone is, the less dense the microstructure is and the more shear friction is, so more shear cracks are generated. That is, the proportion of shear cracks increases with increasing grain size and is positively correlated with the grain size.

As shown in **Figure 11**, the AF value distribution of sandstone with different grain sizes under Brazilian splitting is different: coarse sandstone is 0–90 kHz, medium sandstone is 0–27 kHz, fine sandstone is 0–90 kHz, and siltstone is 0–125 kHz. The RA values of coarse sandstone are 0–800, medium sandstone 0–800, fine sandstone 0–1750, and siltstone 0–600. The main reason is the difference in internal structure, which leads to different deformation and failure modes, and thus the AE signals are different. Siltstone and coarse sandstone produce fewer shear cracks, while coarse and fine sandstone produces more, mainly due to the difference in internal structure, which is not significantly correlated with grain size. The deformation and failure modes are mainly affected by the grain shape.

The microfailure mechanism of sandstone with different grain sizes under the two conditions is the tension-shear mixed failure, which is dominated by tensile failure, with few shear failures. The proportion of shear cracks increases with increasing grain size under uniaxial compression, which is positively correlated with the grain size. However, there is no obvious correlation between the shear crack and grain size under Brazilian splitting.

CONCLUSION

(1) The P-wave velocity, density, compressive strength and tensile strength of weakly cemented sandstones with different grain sizes decrease with the increase of grain size. The pre-peak deformation characteristics are the same, but there are differences after peak stress: ductile failure occurs after the peak for medium and coarse sandstones, while brittle failure occurs after the peak for siltstone and fine sandstones.

(2) The evolution of the AE signal intensity of sandstone with different grain sizes under uniaxial compression and Brazilian splitting is the same, and the distribution in the time domain is nearly normal. The upper limit of the signal intensity and peak frequency of sandstone with different grain sizes are negatively correlated with grain size, and the occurrence of a large amount of high-intensity AE signals can be used as the failure precursor of weakly cemented sandstone.

(3) The damage evolution of sandstone with different grain sizes under uniaxial compression and Brazilian splitting is the same, showing the evolution of low damage-accelerated damage-low damage. However, there are significant differences in the damage increase at the peak load. The smaller the grain size is, the higher the damage increase is. The damage increase is negatively correlated with the grain size.

(4) The microfailure mechanism of sandstone with different grain sizes under the two conditions is the tension-shear mixed failure, which is dominated by tensile failure, with few shear failures. The proportion of shear cracks increases with increasing grain size under uniaxial compression, which is positively correlated with the grain size. However, there is no obvious correlation between the shear crack and grain size under Brazilian splitting.

DATA AVAILABILITY STATEMENT

The original contributions presented in the study are included in the article/Supplementary Material, further inquiries can be directed to the corresponding authors.

AUTHOR CONTRIBUTIONS

BL: Methodology, Writing original draft, Data processing, and Funding acquisition. TZ: Review; Editing, and Funding acquisition. HZ: Review; Editing and Funding acquisition. QY: Review, and Editing.

FUNDING

This work was supported by the Institute of Energy, Hefei Comprehensive National Science Center (No. 21KZS216), the

2021 Startup Foundation for Introducing Talent of Anhui University of Science and Technology (2021yjrc28), the Open Project Program Foundation of Engineering Research Center of underground mine construction, Ministry of Education (No. JYBGCZX2020106) and the Open Fund of State Key Laboratory of Mining Response and Disaster Prevention and Control in Deep Coal Mines (No. SKLMRDPC20KF04). These sources of support are gratefully acknowledged.

REFERENCES

Aggelis, D. G. (2011). Classification of Cracking Mode in Concrete by Acoustic Emission Parameters. *Mech. Res. Commun.* 38, 153–157. doi:10.1016/j.mechrescom.2011.03.007

Atapour, H., and Mortazavi, A. (2018a). The Effect of Grain Size and Cement Content on Index Properties of Weakly Solidified Artificial Sandstones. *J. Geophys. Eng.* 15, 613–619. doi:10.1088/1742-2140/aaa14a

Atapour, H., and Mortazavi, A. (2018b). The Influence of Mean Grain Size on Unconfined Compressive Strength of Weakly Consolidated Reservoir Sandstones. *J. Petroleum Sci. Eng.* 171, 63–70. doi:10.1016/j.petrol.2018.07.029

Bai, Y., Shan, R., Ju, Y., Wu, Y., Sun, P., and Wang, Z. (2020). Study on the Mechanical Properties and Damage Constitutive Model of Frozen Weakly Cemented Red Sandstone. *Cold Regions Sci. Technol.* 171, 102980. doi:10.1016/j.coldregions.2019.102980

Cai, J., and Zou, W. (2020). Triaxial Compressive Failure Characteristics and Constitutive Model Study of Jurassic-Cretaceous Weakly Cemented Sandstone. *Adv. Civ. Eng.* 2020, 1–12. doi:10.1155/2020/8812575

Carbillet, L., Heap, M. J., Baud, P., Wadsworth, F. B., and Reuschlé, T. (2021). Mechanical Compaction of Crustal Analogs Made of Sintered Glass Beads: The Influence of Porosity and Grain Size. *J. Geophys. Res. Solid Earth* 126, 1–25. doi:10.1029/2020JB021321

Chen, Y., Zuo, J., Liu, D., Li, Y., and Wang, Z. (2021). Experimental and Numerical Study of Coal-Rock Bimaterial Composite Bodies under Triaxial Compression. *Int. J. Coal Sci. Technol.* 8, 908–924. doi:10.1007/s40789-021-00409-5

Cheng, S., Guo, Y., Huang, W., and Yin, D. (2017). Experimental Study of Influence Regularity and Mechanism of Particle Size on Mechanical Properties of Red Sandstone. *J. Shandong Univ. Sci. Technol. Nat. Sci.* 36, 8–14. doi:10.16452/j.cnki.sdkjzk.2017.06.002

Dou, L., Yang, K., and Chi, X. (2021). Fracture Behavior and Acoustic Emission Characteristics of Sandstone Samples with Inclined Precracks. *Int. J. Coal Sci. Technol.* 8, 77–87. doi:10.1007/s40789-020-00344-x

Du, F., and Peng, S. S. (2019). Change Rule of Physical and Mechanical Property of Rock Mass in Shendong Mine. *Caikuang yu Anquan Gongcheng Xuebao/Journal Min. Saf. Eng.* 36, 1009–1015. doi:10.13545/j.cnki.jmse.2019.05.019

Eberhardt, E., Stead, D., Stimpson, B., and Read, R. S. (1998). Identifying Crack Initiation and Propagation Thresholds in Brittle Rock. *Can. Geotech. J.* 35, 222–233. doi:10.1139/t97-091

Elfergani, H. A., Pullin, R., and Holford, K. M. (2013). Damage Assessment of Corrosion in Prestressed Concrete by Acoustic Emission. *Constr. Build. Mater.* 40, 925–933. doi:10.1016/j.conbuildmat.2012.11.071

Galouei, M., and Fakhimi, A. (2015). Size Effect, Material Ductility and Shape of Fracture Process Zone in Quasi-Brittle Materials. *Comput. Geotechnics* 65, 126–135. doi:10.1016/j.compgeo.2014.12.010

Gardner, G. H. F., Gardner, L. W., and Gregory, A. R. (1974). Formation Velocity and Density-The Diagnostic Basics for Stratigraphic Traps. *Geophysics* 39, 770–780. doi:10.1190/1.1440465

He, S.-H., Ding, Z., Hu, H.-B., and Gao, M. (2021). Effect of Grain Size on Microscopic Pore Structure and Fractal Characteristics of Carbonate-Based Sand and Silicate-Based Sand. *Fractal Fract.* 5, 152. doi:10.3390/fractalfract5040152

He, W., Hayatdavoudi, A., Shi, H., Sawant, K., and Huang, P. (2019). A Preliminary Fractal Interpretation of Effects of Grain Size and Grain Shape on Rock Strength. *Rock Mech. Rock Eng.* 52, 1745–1765. doi:10.1007/s00603-018-1645-4

Hoek, E., and Bieniawski, Z. T. (1984). Brittle Fracture Propagation in Rock under Compression. *Int. J. Fract.* 26, 276–294. doi:10.1007/BF00962960

Jin, Y., Han, L., Meng, Q., Sanda, S., Zang, H., and Feng, B. (20182018). Mechanical Properties of Grouted Crushed Coal with Different Grain Size Mixtures under Triaxial Compression. *Adv. Civ. Eng.* 2018, 1–13. doi:10.1155/2018/9473947

Kang, F., Li, Y., and Tang, C. a. (2021). Grain Size Heterogeneity Controls Strengthening to Weakening of Granite over High-Temperature Treatment. *Int. J. Rock Mech. Min. Sci.* 145, 104848. doi:10.1016/j.ijrmms.2021.104848

Kong, F., Xue, Y., Qiu, D., Gong, H., and Ning, Z. (2021a). Effect of Grain Size or Anisotropy on the Correlation between Uniaxial Compressive Strength and Schmidt Hammer Test for Building Stones. *Constr. Build. Mater.* 299, 123941. doi:10.1016/j.conbuildmat.2021.123941

Kong, F., Xue, Y., Qiu, D., Li, Z., Chen, Q., and Song, Q. (2021b). Impact of Grain Size or Anisotropy on Correlations between Rock Tensile Strength and Some Rock Index Properties. *Geomech. Eng.* 27, 131–150. doi:10.12989/gae.2021.27.2.131

Li, H., Li, H., Gao, B., Wang, W., and Liu, C. (2017). Study on Pore Characteristics and Microstructure of Sandstones with Different Grain Sizes. *J. Appl. Geophys.* 136, 364–371. doi:10.1016/j.jappgeo.2016.11.015

Li, H., and Li, H. (2017). Mechanical Properties and Acoustic Emission Characteristics of Thick Hard Roof Sandstone in Shendong Coal Field. *Int. J. Coal Sci. Technol.* 4, 147–158. doi:10.1007/s40789-017-0163-4

Liu, B., Huang, J., Wang, Z., and Liu, L. (2009). Study on Damage Evolution and Acoustic Emission Character of Coal-Rock under Uniaxial Compression. *Yanshilixue Yu Gongcheng Xuebao/Chinese J. Rock Mech. Eng.* 28, 3234–3238.

Liu, B., Zhao, Y., Zhang, C., Zhou, J., Li, Y., and Sun, Z. (2021). Characteristic Strength and Acoustic Emission Properties of Weakly Cemented Sandstone at Different Depths under Uniaxial Compression. *Int. J. Coal Sci. Technol.* 8, 1288–1301. doi:10.1007/s40789-021-00462-0

Liu, Q., Sun, Y., and Li, J. (2020). Experimental Study on Seepage Characteristics of Jurassic Weakly Cemented Sandstone under Water-Rock Interaction. *Geofluids* 2020, 1–12. doi:10.1155/2020/8543687

Lyu, X., Zhao, Z., Wang, X., and Wang, W. (2019). Study on the Permeability of Weakly Cemented Sandstones. *Geofluids* 2019, 1–14. doi:10.1155/2019/8310128

Qi, Y., Ju, Y., Yu, K., Meng, S., and Qiao, P. (2022). The Effect of Grain Size, Porosity and Mineralogy on the Compressive Strength of Tight Sandstones: A Case Study from the Eastern Ordos Basin, China. *J. Petroleum Sci. Eng.* 208, 109461. doi:10.1016/j.petrol.2021.109461

Song, Z., Ji, H., Liu, Z., and Sun, L. (2020). Study on the Critical Stress Threshold of Weakly Cemented Sandstone Damage Based on the Renormalization Group Method. *Int. J. Coal Sci. Technol.* 7, 693–703. doi:10.1007/s40789-020-00315-2

Tian, W.-L., Yang, S.-Q., Xie, L.-X., and Wang, Z.-L. (2018). Cracking Behavior of Three Types Granite with Different Grain Size Containing Two Non-coplanar Fissures under Uniaxial Compression. *Archives Civ. Mech. Eng.* 18, 1580–1596. doi:10.1016/j.acme.2018.06.001

Wang, H., Yang, T., and Zuo, Y. (2018). Experimental Study on Acoustic Emission of Weakly Cemented Sandstone Considering Bedding Angle. *Shock Vib.* 2018, 1–12. doi:10.1155/2018/6086583

Wang, Z., Chen, J., Li, W., Wang, Q., Niu, Q., Liu, S., et al. (2020). Relationship between Petrographic Parameters and Physical-Mechanical Properties of Weakly Cemented Sandstones. *Q. J. Eng. Geol. Hydrogeology* 54, qjegh2018–168. doi:10.1144/qjegh2018-168

Wasantha, P. L. P., Ranjith, P. G., Zhao, J., Shao, S. S., and Permata, G. (2015). Strain Rate Effect on the Mechanical Behaviour of Sandstones with Different Grain Sizes. *Rock Mech. Rock Eng.* 48, 1883–1895. doi:10.1007/s00603-014-0688-4

Wu, C., Wang, S., Li, D., and Wang, X. (2020). NMR Experimental Study on Dynamic Process of Pore Structure and Damage Mechanism of Sandstones with Different Grain Sizes under Acid Erosion. *Shock Vib.* 2020, 1–13. doi:10.1155/2020/3819507

Yang, D., Ning, Z., Li, Y., Lv, Z., and Qiao, Y. (2021). *In Situ* stress Measurement and Analysis of the Stress Accumulation Levels in Coal Mines in the Northern Ordos Basin, China. *Int. J. Coal Sci. Technol.* 8, 1316–1335. doi:10.1007/s40789-021-00407-7

You, S., Ji, H., Wang, T., and Song, Z. (2018). Thermal and Mechanical Coupling Effects on Permeability of Weakly Cemented Sandstone. *Emerg. Mater. Res.* 7, 100–108. doi:10.1680/jemmr.16.00082

Yu, M., Li, S., Sun, Q., and Wang, S. (2021). Influence of Grain Size on the Strain-rate-dependent Dynamic Response of Sandstones. *Geomech. Geophys. Geo-energ. Geo-resour.* 7, 1–15. doi:10.1007/s40948-021-00273-2

Yu, M., Wei, C., and Niu, L. (2017). The Coupled Effect of Loading Rate and Grain Size on Tensile Strength of Sandstones under Dynamic Disturbance. *Shock Vib.* 2017, 1–13. doi:10.1155/2017/6989043

Zhao, Y., Liu, B., Yang, Z., Song, G., and Yang, D. (2019). Tensile Strength and Fracture Toughness of Sedimentary Rocks at Different Buried Depths in Shendong Coal Field. *Meitan Xuebao/Journal China Coal Soc.* 44, 1732–1741. doi:10.13225/j.cnki.jccs.2018.9031

Zou, H., Liu, J. F., Bian, Y., Zhou, Z. W., and Zhuo, Y. (2015). Experimental Study on Mechanical and Permeability Properties of Sandstone with Different Granularities. *Yantu Gongcheng Xuebao/Chinese J. Geotech. Eng.* 37, 1462–1468. doi:10.11779/CJGE201508015

Conflict of Interest: The authors declare that the research was conducted in the absence of any commercial or financial relationships that could be construed as a potential conflict of interest.

Publisher's Note: All claims expressed in this article are solely those of the authors and do not necessarily represent those of their affiliated organizations, or those of the publisher, the editors and the reviewers. Any product that may be evaluated in this article, or claim that may be made by its manufacturer, is not guaranteed or endorsed by the publisher.